Pyrrolo-dC oligonucleotides bearing alkynyl side chains with terminal triple bonds: synthesis, base pairing and fluorescent dye conjugates prepared by the azide–alkyne "click" reaction†

Frank Seela*[a,b] and Venkata Ramana Sirivolu[a,b]

Received 17th December 2007, Accepted 1st February 2008
First published as an Advance Article on the web 26th March 2008
DOI: 10.1039/b719459e

5-(Octa-1,7-diynyl)-2′-deoxyuridine was converted into the furano-dU derivative **7** by copper-catalyzed cyclization; the pyrolodC-derivative **3** was formed upon ammonolysis. The bicyclic nucleosides **3** and **7** as well as the corresponding non-cyclic precursors **4** and **6** all containing terminal C≡C bonds were conjugated with the non-fluorescent 3-azido-7-hydroxycoumarin **5** employing the copper(I)-catalyzed Huisgen–Sharpless–Meldal cycloaddition "click reaction". Strongly fluorescent 1*H*-1,2,3-triazole conjugates (**30–33**) are formed incorporating two fluorescent reporters—the pyrdC nucleoside and the coumarin moiety. Oligonucleotides incorporating 6-alkynyl and 6-alkyl 7*H*-pyrrolo[2,3-*d*]pyrimidin-2(3*H*)-one nucleosides (**3** and **2f**) have been prepared by solid-phase synthesis using the phosphoramidite building blocks **10** and **13**; the pyrrolo-dC oligonucleotides are formed during ammonia treatment. The duplex stability of oligonucleotides containing **3** and related derivatives was studied. Oligonucleotides with terminal triple bonded nucleosides such as **3** are more stabilizing than those lacking a side chain with terminal unsaturation; open-chain derivatives (**4**) are even more efficient. The click reaction was also performed on oligonucleotides containing the pyrdC-derivative **3** and the fluorescence properties of nucleosides, oligonucleotides and their coumarin conjugates were studied.

Introduction

Fluorescent reporter groups are widely used to explore the structure, dynamics and interactions of nucleic acids. As canonical bases of nucleic acids are non-emissive, numerous fluorescent nucleobase analogues have been synthesized and incorporated into DNA.[1a] Among the modified purine derivatives, 2-amino purines,[1b] 2-amino- and 2-hydroxy pyrrolo[2,3-*d*]pyrimidines[2–4] as well as 1,N^6-etheno compounds[5,6] are all fluorescent. Various cytosine nucleosides, such as etheno-dC[7,8] and pyrrolo-C (pyrC) or pyrrolo-dC (pyrdC) develop significant fluorescence. PyrC (**2a**, **2b**) or pyrdC (**2c**, **2d**) (Scheme 1) are related to the pyrrolo[2,3-*d*]pyrimidine nucleoside **1**,[4] which is strongly fluorescent. PyrC/dC are prepared from the furano-U or furano-dU,[9–11] which are accessible from the 5-alkynyl compounds by cyclization with copper iodide. The bicyclic furano pyrimidine nucleoside analogues posses significant biological activity against *Varicella Zoster* virus.[12,13] Treatment of the furo[2,3-*d*]pyrimidine nucleosides (*e.g.* **7**) with ammonia generates the pyrrolo[2,3-*d*]pyrimidine nucleosides (*e.g.* **3**), a reaction which takes place during oligonucleotide deprotection. An alternative synthetic route makes use of the low nucleophilicity of the pyrrol nitrogen allowing the regioselective nucleobase anion glycosylation[6] at nitrogen N1, as was exemplified on compound **2a**. PyrC or pyrdC has been incorporated into oligoribo- and oligodeoxyribonucleotides using the standard protocol of solid-phase synthesis.[10] Fluorescent 6-unsubstituted 7*H*-pyrrolo[2,3-*d*]pyrimidin-2(3*H*)-one derivatives and related bicyclic analogues were reported to develop stable base pairs with dG.[14,15] A tridentate base pair is formed between compound **2c** and dG which can mimic the dC–dG base pair.[9] Nucleoside **2d** has been used to study nucleic acid duplex and triplex formation or to probe DNA/RNA interactions with proteins.[16–21]

This manuscript reports on pyrdC-derivatives bearing side chains at the 6-position with a terminal triple bond. This functionality allows further derivatisation of the whole molecule by the copper(I)-catalyzed Huisgen–Sharpless–Meldal 1,3-dipolar cycloaddition reaction, the so-called "click" reaction.[22–24] This protocol is orthogonal to other reactions and can be performed efficiently in aqueous media with high functional group tolerance. Earlier investigations by our laboratory have demonstrated that a set of all four canonical bases, pyrimidines and purines—the latter in the form of their 7-deaza derivatives—can be functionalized by this route.[25–27] The terminal C≡C bonds of the pyrdC-derivative **3** and its open-chain analogue **4** were conjugated with the non-fluorescent azido–coumarin **5** generating strongly fluorescent 1,4-disubstitued 1*H*-1,2,3-triazole conjugates (Scheme 2). These molecules contain two fluorescent moieties: the pyrrolo-dC base and the coumarin dye. The "click" reaction was also performed on the oligonucleotide level. After hybridization the duplex DNA contains one fluorescent reporter (pyrdC) being part of the base pair stack while the other fluorescent residue (coumarin)

[a]*Laboratory of Bioorganic Chemistry and Chemical Biology, Center for Nanotechnology, Heisenbergstraße 11, 4814, Münster, Germany. E-mail: Frank.Seela@uni-osnabrueck.de, Seela@uni-muenster.de; Web: www.seela.net; Fax: +49 (0)251 53 406 857; Tel: +49 (0)251 53 406 500*
[b]*Laboratorium für Organische und Bioorganische Chemie, Institut für Chemie, Universität Osnabrück, Barbarastraße 7, 49069, Osnabrück, Germany*

† Electronic supplementary information (ESI) available: Table 5. See DOI: 10.1039/b719459e

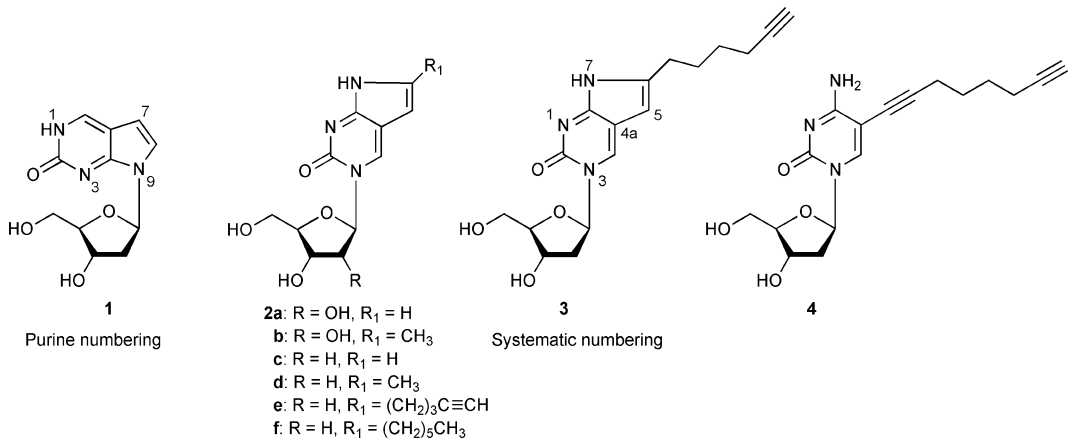

Scheme 1 Structures of nucleosides.

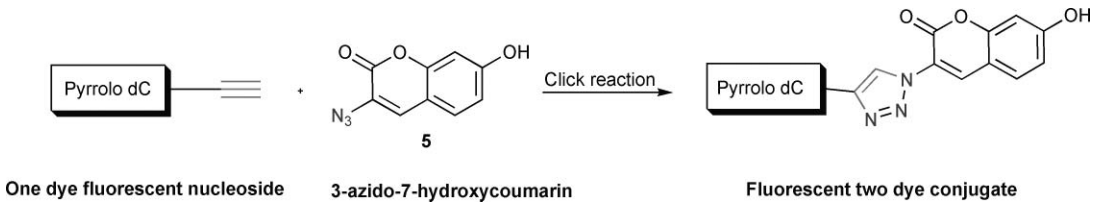

Scheme 2 Copper(I)-catalyzed alkyne–azide cycloaddition.

is protruding into the major groove of the DNA duplex. The duplex stability of modified base pairs was compared with those incorporating dC–dG.

Results and discussion

1. Synthesis and properties of monomers

The syntheses of 5-alkynylated 2′-deoxyuridine **6** and the 5′-*O*-(4,4′-dimethoxytrityl) derivatives **8** and **11** have already been reported from our laboratory using the Sonogashira cross-coupling reaction followed by dimethoxytritylation.[25,26] Earlier, a one-pot preparation of bicyclic furano nucleoside **7** was described; however, as the yield was below 20%[28] the 5-(octa-1,7-diynyl)-2′-deoxyuridine intermediate **6** was isolated first, which was then cyclized in the presence of CuI to give the 6-hexynyl-3*H*-furo[2,3-*d*]pyrimidin-2-one nucleoside **7** in 87% yield, which undergoes conversion in aqueous ammonia to form the 6-hexynyl-7*H*-pyrrolo[2,3-*d*]pyrimidin-2(3*H*)-one nucleoside **3** in 90% yield (Scheme 3). An alternative synthetic route was reported by our laboratory for the synthesis of the pyrC-derivative **2a** using the regioselective glycosylation of the 7-deazapurine-2-one at nitrogen-1.[6] Compound **2e** was prepared using the same cyclization reaction as reported above and their fluorescence properties were investigated.[6]

To study the effect of 6-alkynyl and 6-alkyl substitution of pyrdC on the DNA duplex stability, oligonucleotides containing **3** and **2f** were synthesized. For that purpose the phosphoramidite building blocks **10** and **13** were prepared and employed in solid-phase oligonucleotide synthesis. Two routes were performed for the preparation of the dimethoxytrityl derivative **9**. The first method starts with the dimethoxytritylation of the 6-hexynyl 3*H*-furo[2,3-*d*]pyrimidin-2-one nucleoside **7**, while the second begins

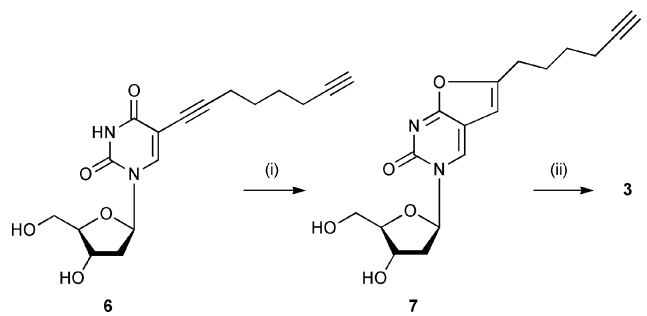

Scheme 3 *Reagents and conditions*: (i) Et_3N/MeOH, CuI, reflux 70 °C; (ii) 25% aq. NH_3, overnight, r.t.

with the cyclization of the 5-octa-1,7-diynylated dimethoxytrityl derivative **8** to form **9** (85% yield). In a similar way the 5-oct-1-ynylated dimethoxytrityl derivative **11** was cyclized into **12** in 87% yield. The above compounds were further transformed into the phosphoramidite building blocks **10** and **13** by phosphitylation reaction using chloro-(2-cyanoethoxy)-*N*,*N*-diisopropylaminophosphine (Scheme 4). For comparison the phosphoramidite building block of **2d** was prepared according to the reported procedure.[20]

The target compounds and all intermediates were characterized by ^{1}H, ^{13}C NMR and ^{31}P-NMR spectroscopy as well as by elemental analyses. The cyclized **7** shows a signal (6.44 ppm) consistent with the chemical shift of a vinyl proton and no signals beyond 10 ppm, revealing the absence of an imino proton. The presence of an NH signal at 11 ppm indicates the formation of pyrrolo-dC derivative **3**. The ^{13}C NMR signals were assigned on the basis of related compounds (**2a**, **2d**, **2e**), which were assigned earlier[6,11] by their gated-decoupled spectra, and are displayed in

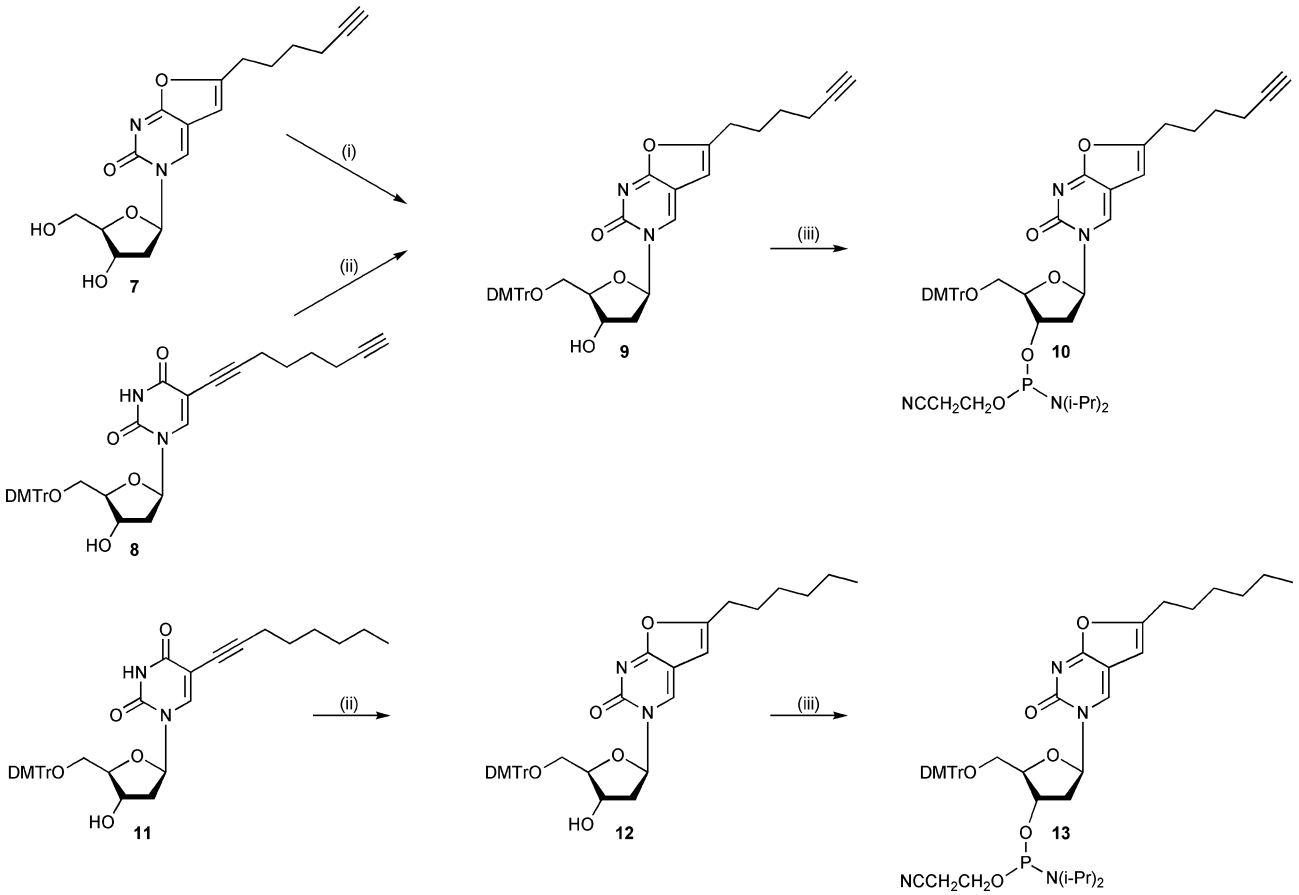

Scheme 4 *Reagents and conditions*: (i) DMTr-Cl, pyridine, 6 h, r.t.; (ii) Et_3N/MeOH, CuI, reflux 70 °C; (iii) $^{i}Pr_2NP(Cl)OCH_2CH_2CN$, $^{i}Pr_2EtN$, CH_2Cl_2, 45 min, r.t.

Table 1. A significant chemical shift difference is observed for the C2 and C4 signals (purine numbering is used) in the ^{13}C NMR spectra of pyrrolo-dC **3** and its furano precursor **7**. Moreover, C4, which is connected to the pyrdC, appears at 159 ppm, while C4 of the furano compound **7** is in the range of 171–172 ppm. The assignments of the C1′ and C4′ sugar signals uses differences in the coupling constants taken from the gated-decoupled spectra.[6] The side chain of **3** shifts C8 upfield (14) ppm when compared to the methyl compound.[6]

2. Synthesis and characterization of oligonucleotides

Oligonucleotide synthesis was carried out on solid phase with an ABI 392–08 synthesizer at a 1 μmol scale employing the

Table 1 ^{13}C-NMR chemical shifts of modified nucleosides and their derivatives measured in d_6-DMSO at 298 K

	C2[a] / C2[b]	C4[a] / C7a[b]	C5[a] / C4a[b]	C6[a] / C4[b]	C7[a] / C5[b]	C8[a] / C6[b]	C≡C[c] / triazole[d]		C1′	C2′	C3′	C4′	C5′
2a[6]	154.1	158.7	107.4	137.3	100.5	127.4	—	—	91.1	74.9	68.4	84.1	59.8
2d[6]	153.7	159.2	108.9	134.0	96.8	137.6	—	—	86.5	41.2	69.8	87.6	60.9
2e[6]	153.7	159.1	108.6	134.5	96.5	141.1	83.7	71.6	86.6	41.3	69.6	87.6	61.9
3	153.8	159.2	108.7	134.5	96.4	142.0	84.3	71.3	86.6	41.3	69.9	87.7	61.0
7	157.9	171.2	106.3	136.8	99.9	153.7	84.2	71.3	87.3	41.2	69.6	88.0	60.7
9	158.0	171.2	106.2	136.4	99.3	153.7	84.2	71.3	86.0	41.2	69.0	87.3	62.5
12	159.0	172.0	107.0	137.2	99.9	154.5	—	—	86.7	42.0	69.8	88.0	63.3
30	158.3	171.3	106.6	137.0	100.0	154.7	147.0	123.0	87.6	41.3	69.8	88.2	60.9
31	153.9	159.2	108.8	134.5	96.5	142.2	146.9	122.8	86.7	41.3	69.9	87.7	61.1
32	149.4	—	—	161.7	98.9	142.7	146.8	122.8	84.6	[e]	70.1	87.5	60.9
33	153.5	—	—	164.3	90.4	143.5	146.8	122.8	85.2	[e]	70.1	87.4	61.0

[a] Purine numbering. [b] Systematic numbering. [c] Triple bond carbons for compounds **2e**, **3**, **7**, **9**. [d] Triazole carbons for compounds **30–33**. [e] Superimposed by the signal of DMSO-d_6.

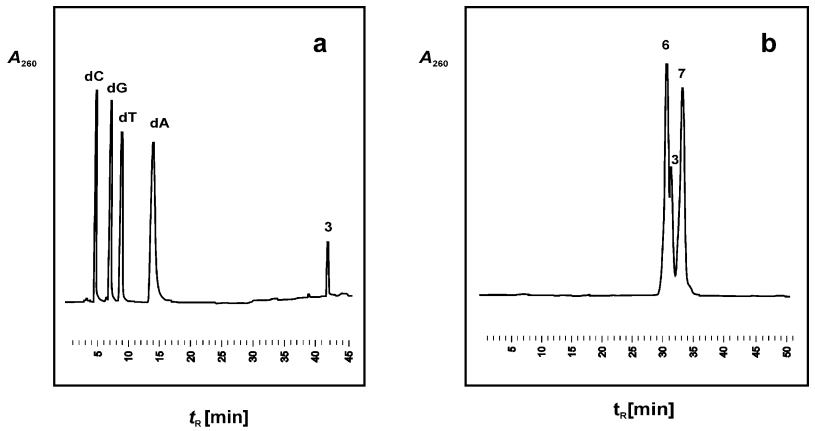

Fig. 1 HPLC profile a) of the reaction products obtained after enzymatic hydrolysis of the oligomer 5′-d(AGT AT**3** GAC CTA) with snake venom phosphodiesterase and alkaline phosphatase in 0.1 M Tris-HCl buffer (pH 8.5) at 37 °C, b) of an artificial mixture of nucleosides **3**, **6** and **7**. Column: LiChrosphere 100 RP-18 (5 µm). The following solvent systems were used: MeCN (A) and 0.1 M (Et_3NH)OAc (pH 7.0)/MeCN 95:5 (B); gradient for **a**: 25 min 100% B, 50 min 0–50% A in B; gradient for **b**: 50 min 5–60% A in B.

synthesized phosphoramidites **10**, **13** as well as standard building blocks. The coupling yields were always higher than 95%. The synthesis of oligonucleotides was performed by employing the DMT-on mode. After cleavage from the solid support, the oligomers were deprotected in 25% aqueous ammonia solution for 14–16 h at 60 °C. The purification of 5′-dimethoxytrityl oligomers was carried out on reverse-phase HPLC (see Experimental section). The base composition of the oligonucleotides was determined by tandem enzymatic hydrolysis (for details see Experimental section). The HPLC profile of the reaction products obtained after enzymatic digestion clearly demonstrates that the newly incorporated nucleoside **3** migrate much slower than the canonical DNA constituents (Fig. 1a). The molecular masses of the oligonucleotides were determined by MALDI-TOF Biflex-III mass spectrometry (Bruker Saxonia, Leipzig, Germany) and Applied Biosystems Voyager DE PRO with 3-hydroxypicolinic acid (3-HPA) as a matrix. The detected masses were identical with the calculated values (see ESI, Table 5†). During deprotection of oligonucleotides the incorporated furano pyrimidines were converted into pyrrolo pyrimidines (Scheme 5). In order to confirm this, the structure of the modified nucleoside was not altered during oligonucleotide synthesis. The mobility of the nucleosides on reverse-phase HPLC refers to the hydrophobic character of the side chains of the nucleosides with compound **7** as the slowest migrating compound when compared with the nucleosides **6** and **3** (Fig. 1b).

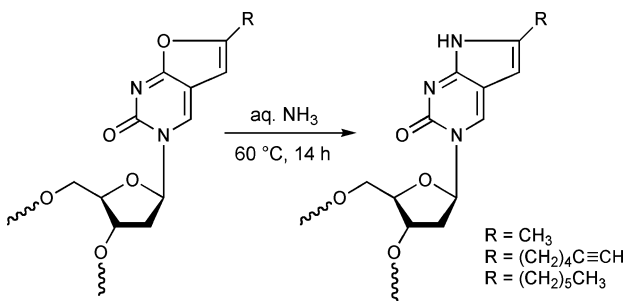

Scheme 5 Conversion of the furano moiety of compound (**7**) into the pyrrole ring system (**3**) after treatment with aqueous NH_3.

3. The duplex stability of oligonucleotides incorporating base pairs formed by the bycylic compounds 3, 2f, 2d and the open-chain analogue 5-(octa-1,7-diynyl)-2′-deoxycytidine (4)

The duplex stability of non-self complementary duplexes containing various 6-substituted pyrrolo-dC nucleosides was investigated (Table 2). For that the duplex 5′-d[TAG GTC AAT ACT] (**14**) and 3′-d[ATC CAG TTA TGA] (**15**) was used as a reference and the modified nucleosides shown in Scheme 6 were incorporated in the place of dC.

A single replacement of pyrrolo-dC nucleosides shows a positive influence on the DNA duplex stability with a tendency of higher stabilization for the open-chain compounds (Scheme 6). The nucleoside conjugate **31** containing the 1,2,3-triazole moiety as well as the coumarin dye residue was only slightly destabilized, showing that the bulky side chain does not interfere with base-pairing significantly. To study the effect of multiple incorporations of the pyrrolo-dC nucleosides and corresponding open-chain compounds, a series of oligonucleotides was prepared by incorporating the modified bases at different positions (Table 2). From this a significant difference in the T_m values was observed. It is apparent that the replacement of the canonical 2′-deoxycytidine within DNA duplex by the side chain derivatives leads to the following conclusions. (i) The open-chain compound **4** forms a more stable base pair with dG than the bicyclic pyrrolo-dC derivative **3**. (ii) The DNA duplexes containing a terminal triple bond in the side chain (nucleoside **3**) are more stable than that of **2f** without terminal triple bond. The higher stability of the pyrdC-derivative **3** compared to its saturated analogue **2f** results from the better solvation of the side chain in aqueous solution. It is likely that the triple bond acts as proton acceptor while the terminal proton is a potential H-donor. Thus, water molecules can interact with the side chain terminus by hydrogen bonding which is supported by the fact that the saturated compound **2f** does not show such favorable properties. A similar phenomenon was already observed for the corresponding 2′-deoxyuridine derivatives.[25]

Next, the mismatch formation was studied by incorporating compound **3** against the four canonical nucleosides. For that a similar set of experiments were performed by using a standard

Table 2 T_m values of oligonucleotide duplexes containing the pyrrolo-dC nucleosides **3**, **2f**, **2d** and the open-chain 2′-deoxycytidine derivative **4** located opposite dG[a]

Duplex	T_m/°C	ΔT_m
5′-d(TAG GTC AAT ACT) (**14**)	50	—
3′-d(ATC CAG TTA TGA) (**15**)		
5′-d(TAG GT**3** AAT ACT) (**16**)	52	+2
3′-d(ATC CAG TTA TGA) (**15**)		
5′-d(TAG GTC AAT ACT) (**14**)	47	−3
3′-d(AT**3** **3**AG TTA TGA) (**22**)		
5′-d(TAG GT**3** AAT ACT) (**16**)	49	−1
3′-d(AT**3** **3**AG TTA TGA) (**22**)		
5′-d(TAG GT**31** AAT ACT) (**21**)	48	−2
3′-d(ATC CAG TTA TGA) (**15**)		
5′-d(TAG GT**4** AAT ACT) (**19**)	53	+3
3′-d(ATC CAG TTA TGA) (**15**)		
5′-d(TAG GTC AAT ACT) (**14**)	55	+5
3′-d(AT**4** **4**AG TTA TGA) (**23**)		
5′-d(TAG GT**4** AAT ACT) (**19**)	57	+7
3′-d(AT**4** **4**AG TTA TGA) (**23**)		
5′-d(TAG GT**2f** AAT ACT) (**17**)	51	+1
3′-d(ATC CAG TTA TGA) (**15**)		
5′-d(TAG GTC AAT ACT) (**14**)	44	−6
3′-d(AT**2f** **2f**AG TTA TGA) (**24**)		
5′-d(TAG GT**2f** AAT ACT) (**17**)	45	−5
3′-d(AT**2f** **2f**AG TTA TGA) (**24**)		
5′-d(TAG GT**2d** AAT ACT) (**18**)	51	+1
3′-d(ATC CAG TTA TGA) (**15**)		
5′-d(TAG GT**X** AAT ACT) (**20**)	53	+3
3′-d(ATC CAG TTA TGA) (**15**)		

[a] Measured at 260 nm in 1 M NaCl, 100 mM $MgCl_2$ and 60 mM Na-cacodylate (pH 7.0) with 5 μM single-strand concentration. **X** = 5-Propynyl-2′-deoxycytidine.

oligonucleotide containing pyrrolo-dC nucleoside **3** 3′-d(ATC CAG **3**TA TGA) **26**. The complementary strands are modified in such a way that the modified base located opposite to dA, dC, dT or dG. All mismatches led to a decrease of the duplex stability compared to the **3**–dG base pair. From Table 3, it is concluded that pyrdC (**3**) shows a higher base discrimination than dC. Nevertheless, duplexes incorporating pyrdC (**3**) generally showed higher T_m-values against canonical nucleosides than those containing dC. This might be caused by the increased stacking interactions due to the larger surface area of the pyrdC base compared to dC as well as the stabilizing effect of the side chain.

Table 3 T_m values and thermodynamic data of oligonucleotide duplexes containing the nucleoside **3** located opposite canonical nucleosides[a]

Duplex	T_m/°C	ΔT_m	$\Delta G°_{310}$/kcal mol^{-1}
5′-d(TAG GTC **A**AT ACT) (**14**)	34	—	−7.3
3′-d(ATC CAG **C**TA TGA) (**25**)			
5′-d(TAG GTC **A**AT ACT) (**14**)	37	+3.0	−7.7
3′-d(ATC CAG **3**TA TGA) (**26**)			
5′-d(TAG GTC **T**AT ACT) (**27**)	36	—	−7.6
3′-d(ATC CAG **C**TA TGA) (**25**)			
5′-d(TAG GTC **T**AT ACT) (**27**)	39	+3.0	−8.0
3′-d(ATC CAG **3**TA TGA) (**26**)			
5′-d(TAG GTC **G**AT ACT) (**28**)	56	—	−13.0
3′-d(ATC CAG **C**TA TGA) (**25**)			
5′-d(TAG GTC **G**AT ACT) (**28**)	54	−2.0	−12.1
3′-d(ATC CAG **3**TA TGA) (**26**)			
5′-d(TAG GTC **C**AT ACT) (**29**)	32	—	−6.9
3′-d(ATC CAG **C**TA TGA) (**25**)			
5′-d(TAG GTC **C**AT ACT) (**29**)	35	+3.0	−7.3
3′-d(ATC CAG **3**TA TGA) (**26**)			

[a] Measured at 260 nm in 1 M Nacl, 100 mM $MgCl_2$ and 60 mM Na-cacodylate (pH 7.0) with 5 μM single-strand concentration.

4. Photophysical properties of pyrdC-derivatives and their coumarin conjugates formed by the copper(I)-catalyzed azide–alkyne cycloaddition ("click reaction"); one dye *vs* two dyes fluorescence

The bicyclic furano nucleoside **7** and its corresponding pyrdC analogue **3** exhibit a strong purple luminescence on TLC plates under the UV lamp. Fluorescence spectra of compound **7** shows

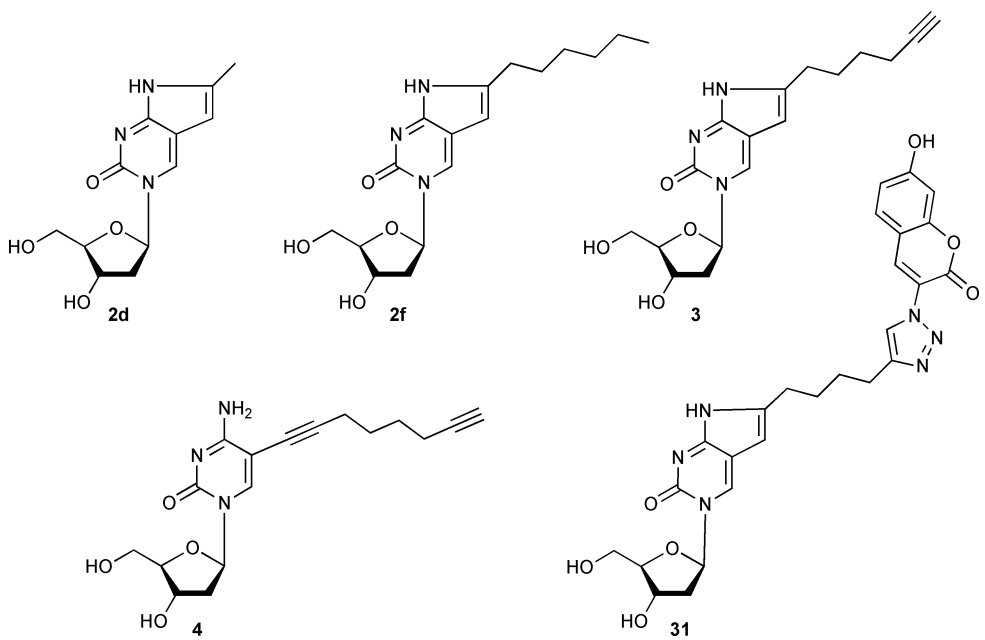

Scheme 6

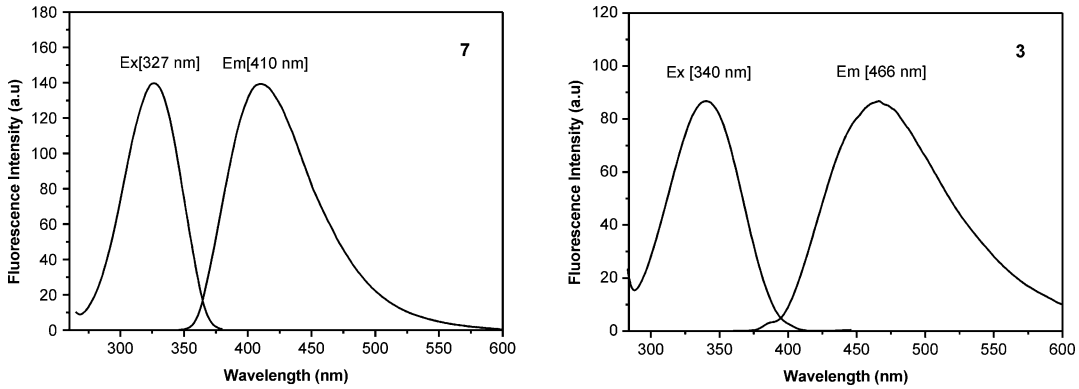

Fig. 2 The emission and excitation spectra of nucleosides **7** and **3** measured at room temperature in bi-distilled water.

an excitation maximum at 327 nm with an emission at 410 nm, where as for the nucleoside **3** longer excitation and emission wavelengths were observed (excitation, 340 nm; emission, 466 nm). A representative emission curves for **7** and **3** are shown in Fig. 2. Also, the Stokes shift is increased from **7** ($\Delta\lambda$ = 83 nm) to **3** ($\Delta\lambda$ = 126 nm). The fluorescence quantum yield (Φ) of **3** in bi-distilled water was determined to be 0.05, which is almost similar to that observed for **7** (0.06). The introduction of a side chain at the 6-position of **3** does not influence the quantum yield significantly when compared to the unsubstituted **2a**, but shifts the excitation as well as the emission maxima to longer wavelength (Table 4).[29]

Although pyrrolo-dC (**3**) and its alkynyl derivatives show significant fluorescence, their extinction coefficients and quantum yields are low when compared to fluorescent dyes like coumarins. Therefore, we intended to conjugate a fluorescent dye to the pyrdC derivative bearing an alkynyl side chain. This would allow to detect possible quenching effects of stacked (pyrdC **3**) and non-stacked (coumarin) fluorescence reporters within ss-oligonucleotides or duplex DNA. The modified version of Huisgen 1,3-dipolar cycloaddition[22] so called "click" chemistry is used for the dye conjugation. Recently, the Sharpless[23] and the Meldal groups[24] demonstrated this chemistry for the functionalization of alkynylated compounds with different azides. The reaction proceeds *via* copper(I)-catalyzed 1,3-dipolar cycloaddition of a terminal alkyne to an organic azide resulting in the exclusive formation of 1,4-disubstituted-1,2,3-triazole. The advantage of this reaction is its insensitivity to oxygen, water and tolerance to a variety of functional groups, which has emerged as the most versatile reaction and found many applications in nucleic acids,[31–33] carbohydrates,[34] drug discovery, polymers and surface chemistry.[35–37]

Moreover, the click reaction is used in biological systems[38,39a] as the azide and alkyne components are unreactive towards biological molecules and the extremely stable 1,2,3-triazole product can have only small interactions with biological structures. The stacking of 1,2,3-triazoles in the major groove of DNA led to slightly enhanced duplex stability.[39b] The 1,2,3-triazole coumarin formed from the terminal alkynes and 3-azido coumarins is found to be highly fluorescent.[40] Among many fluorophores, coumarin derivatives have been extensively studied because of their photophysical properties. Coumarins were used as potential fluorescent probes to investigate the structural dynamics of DNA,[41] for the specific labeling of nucleic acids[42] and mainly as nucleobase-specific quenchers.[43] The derivatives of 7-hydroxycoumarin are generally good fluorophores that are used as dyes for the blue spectra region. The presence of electron-donating groups at the 7-position of 3-azido coumarins show a strong enhancement in the fluorescence.[40] Moreover, it is well documented that the fluorescence properties of coumarin derivatives are pH dependent. Different absorption and emission bands can be observed at various pH values.

Table 4 Photophysical data of the base modified nucleosides[a]

Compound	Excitation/nm	Emission/nm	Quantum yield (Φ)
2a	336	450	0.06
3	340	466	0.05
7	327	410	0.06

[a] Measured in H_2O; quantum yields were determined using quinine sulfate in 0.1 N H_2SO_4 as standard with $\Phi = 0.53$.[30]

The nucleosides **7** and **3** containing terminal C≡C bonds were selectively conjugated with the azide residue of the coumarin dye **5** in the presence of copper sulfate and sodium ascorbate to form the strongly fluorescent 1,4-disubstituted 1,2,3-triazole products **30** and **31** in 82 and 85% yields. In a similar way the open-chain nucleoside–coumarin conjugates **32** (81%) and **33** (61%) were prepared by the copper(I)-catalyzed cycloaddition reaction between 5-(octa-1,7-diynyl)-2′-deoxyuridine (**6**)[25] or 5-(octa-1,7-diynyl)-2′-deoxycytidine (**4**)[27] with **5** (Scheme 7).

The "click" products were identified by comparing their ^{1}H NMR spectra with those of the starting compounds. The terminal side chain proton of the triple bond of **3** (2.75 ppm) and **7** (2.67 ppm) disappeared and newly formed triazole vinyl proton signals of **30** and **31** are now present in the range of 8–9 ppm. Moreover, the ^{13}C spectra shows the absence of terminal C≡C carbon atom signals; the newly associated triazole carbons were found at δ_{C4} = 147 ppm, δ_{C5} = 123 ppm (Table 1). The large difference in triazole carbons for compounds **30–33** ($\Delta\ \delta_{C4}$–δ_{C5} = 24–25 ppm) indicates the chemoselective formation of the 1,4-disubstituted triazole, which is in agreement with previous reports.[44,45] Moreover, the resonance of the triazole ring carbons is clearly evidenced by ^{1}H,^{13}C distortionless enhancement by polarization transfer (DEPT) 135 NMR spectroscopy, not displaying a signal for quaternary carbon (δ_{C4}) and inverted signals of triazole carbon (δ_{C5}) at around 123 ppm.

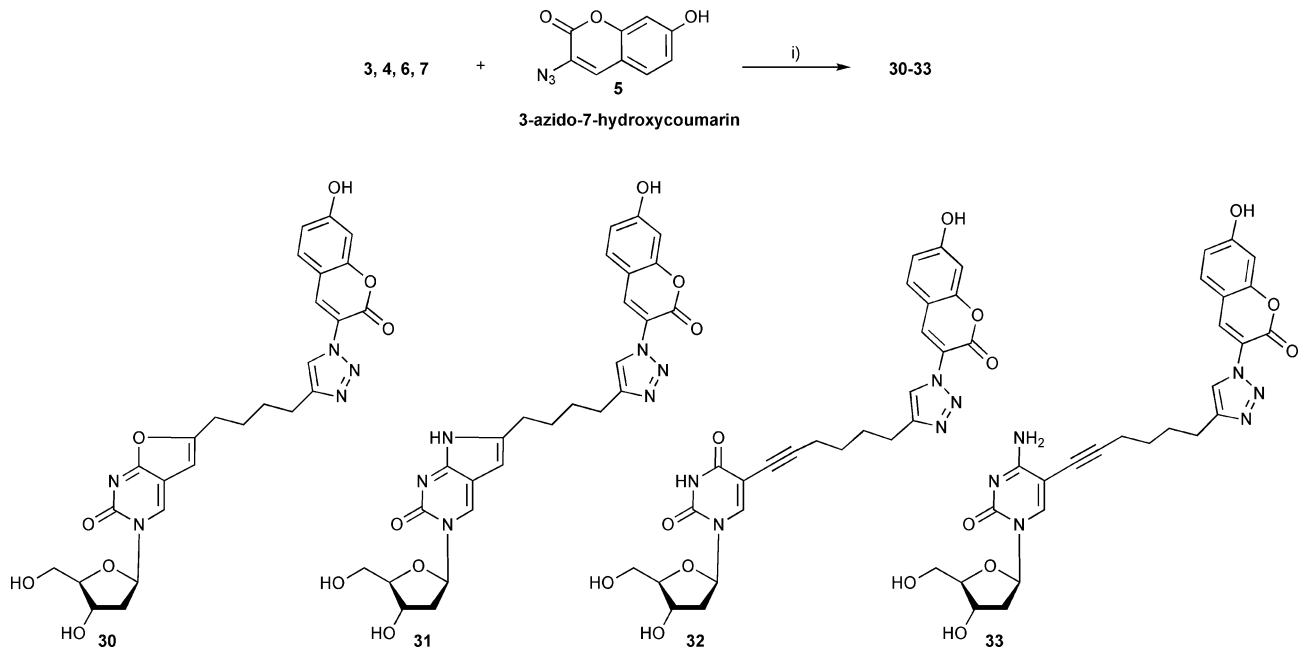

Scheme 7 *Reagents and conditions*: (i) $CuSO_4$, Na-ascorbate, THF–H_2O–*t*-BuOH (3:1:1), r.t.

The mobility of the pyrrolo-dC **31** and the open-chain click nucleoside **33** in reverse-phase HPLC was determined by injecting an artificial mixture of the starting materials and products onto the column; the starting 3-azido-7-hydroxycoumarin (**5**) moves much slower when compared to **3**, **31** (Fig. 3a) and **4**, **33** (Fig. 3b)

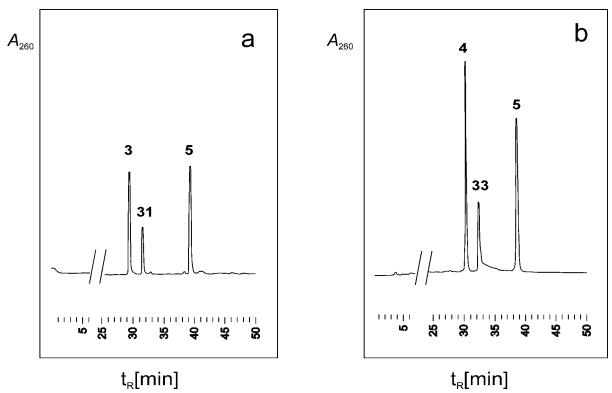

Fig. 3 HPLC profile a) of the artificial mixture of compounds **3**, **5** and **31**, b) of the artificial mixture of compounds **4**, **5** and **33** on a RP-18 (200 × 10 mm) column. The following solvent systems were used: MeCN (A) and 0.1 M (Et_3NH)OAc (pH 7.0)/MeCN 95:5 (B). Gradient 0–50 min 0–50% A in B.

At first, the UV-Vis absorption spectra of terminal alkynyl nucleosides (**3**, **4**, **6**, **7**) and their dye conjugates (**30–33**) were measured (Fig. 4). It is apparent that in the case of open-chain nucleoside–coumarin derivatives **32** and **33** (Fig. 4c,d) a clear differentiation in the absorption bands of the octadiynyl base and coumarin dye can be made. For the furano conjugate (**30**, Fig. 4a), there is only a slight difference in the absorption maxima of furano base when compared to the dye, where as in the case of pyrrolo-dC dye conjugate (**31**, Fig. 4b) the UV absorptions of the pyrdC base and the coumarin dye overlap. So for all the nucleoside–coumarin conjugates the coumarin excitation wavelength around 347 nm is used in the fluorescence experiments which were performed in water.

Next, the fluorescence properties of nucleoside–coumarin 1,2,3-triazolyl conjugates **30** and **31** were studied and compared to the starting nucleosides. The fluorescence emission maxima for all coumarin dye conjugates are almost identical. Differences are observed in the excitation spectra which resulted from the different UV absorptions of the open-chain and bicyclic analogs. The pyrdC–coumarin conjugate **31** has an excitation maximum at 350 nm with an emission at 476 (Stokes shift of 126 nm) (Fig. 5), while the furano–coumarin conjugate **30** has an excitation maximum at 338 nm with a strong emission at 474 nm with a Stokes shift of 136 nm. The Stokes shifts of pyrrolo-dC nucleosides **3** and **31** are almost identical. However, in the case of furano nucleosides **7** and its conjugate **30** there is a large shift in the emission wavelength (from 410 nm to 474 nm) and also a large Stokes shift difference is observed. The fluorescence quantum yields of **30** and **31** in bi-distilled water were determined to be 0.15 and 0.18, which are significantly higher than that of the starting nucleosides **7** (0.06) and **3** (0.05) (Table 4). The solvent pH strongly influences the fluorescence of the dye conjugates. At neutral or lower pH values the possible generation of highly fluorescent phenolate anions was minimized.

Next, the corresponding open-chain derivatives of the mono cyclic nucleoside–dye conjugates **32** and **33** were investigated (Fig. 5). From the fluorescence spectra of nucleoside–coumarin conjugates, an excitation maxima observed at around 398 nm corresponds to that of coumarin dye. The two excitation wavelengths (345 and 392 nm) of coumarins is due to the presence of neutral as well as phenolate anionic species in the solution,[46] while at the alkaline pH value predominantly the phenolate anionic structure is observed with the excitation at 392 nm. The fluorescence quantum yield of 2′-deoxyuridine–dye conjugate **32** (0.32) is higher than that of 2′-deoxycytidine conjugate **33** (0.22). Moreover, the

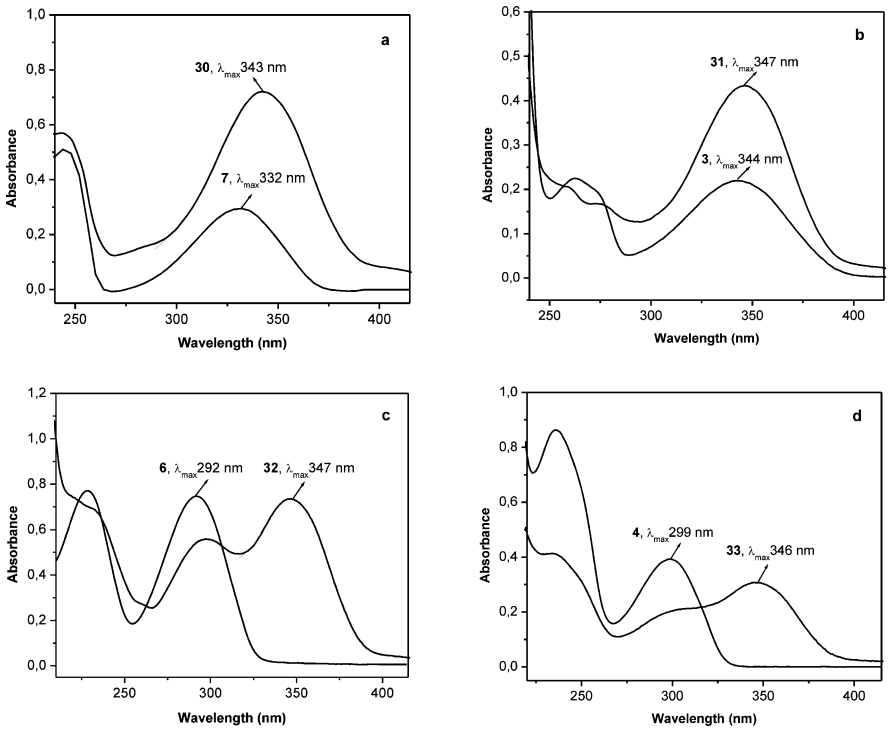

Fig. 4 UV-Vis spectra of a) furano compound **7** and its dye conjugate **30**, b) pyrdC **3** and its dye conjugate **31**, c) 5-octadiynyl-2′-deoxyuridine (**6**) and its dye conjugate **32**, d) 5-octadiynyl-2′-deoxycytidine (**4**) and its dye conjugate **33** measured in methanol.

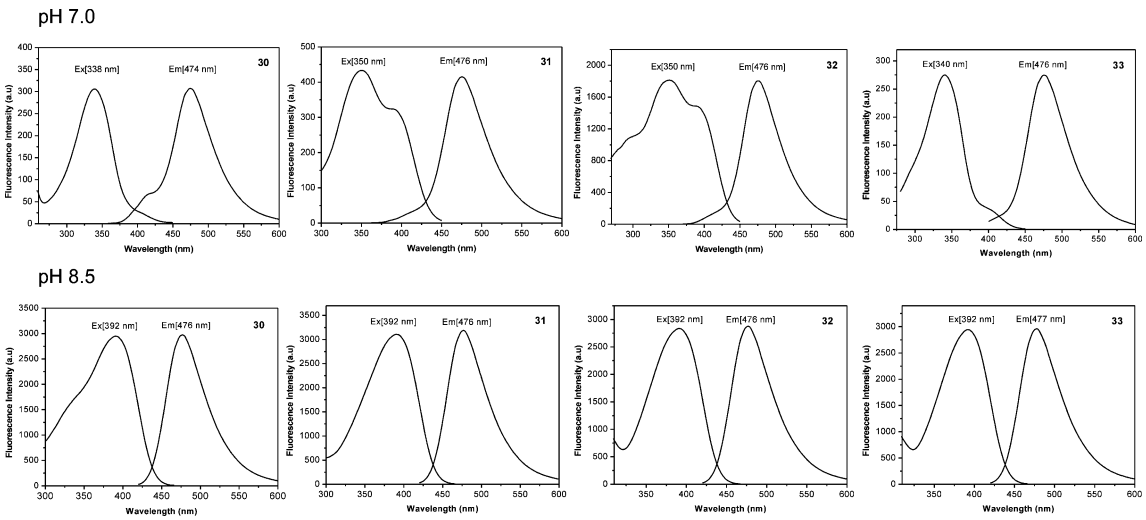

Fig. 5 The emission and excitation spectra of the bicyclic furano nucleoside–coumarin conjugate **30**, the pyrrolo-dC–coumarin conjugate **31**, the open-chain 2′-deoxyuridine–coumarin conjugate **32** and the 2′-deoxycytidine–coumarin conjugate **33** measured in water (pH 7.0, upper row) and 0.1 M Tris-HCl buffer (pH 8.5, lower row).

open-chain coumarin dye conjugates have higher quantum yields than the corresponding cyclic compounds **30** (0.15) and **31** (0.18). The quantum yield of fluorescence for all the nucleosides was determined relative to quinine sulfate in 1.0 N H_2SO_4.

Most of the fluorophores have molar extinction coefficients at their wavelength of maximum absorption ranging between 5000 and 200 000 cm^{-1} M^{-1}.[47] Fluorescence intensity per dye molecule is proportional to the product of extinction coefficient (ε) and quantum yield (Φ). For comparison, the molar extinction coefficients of the nucleoside conjugates **30–33** were measured in methanol. The following values are found: **30** (342 nm 23 000), **31** (346 nm 17 000), **32** (346 nm 21 300), **33** (345 nm 11 000). From these data it is apparent that the extinction coefficient of the pyrrolo-dC coumarin conjugate **31** is higher when compared to that of the open-chain derivative **33**, however a higher quantum yield was observed for the latter.

5. Influence of one dye and two dye pyrrolo-dC derivatives on the fluorescence properties of ss- and ds-DNA

In the following the fluorescence properties of pyrrolo-dC nucleoside **3** and its coumarin conjugate **31** were studied at the

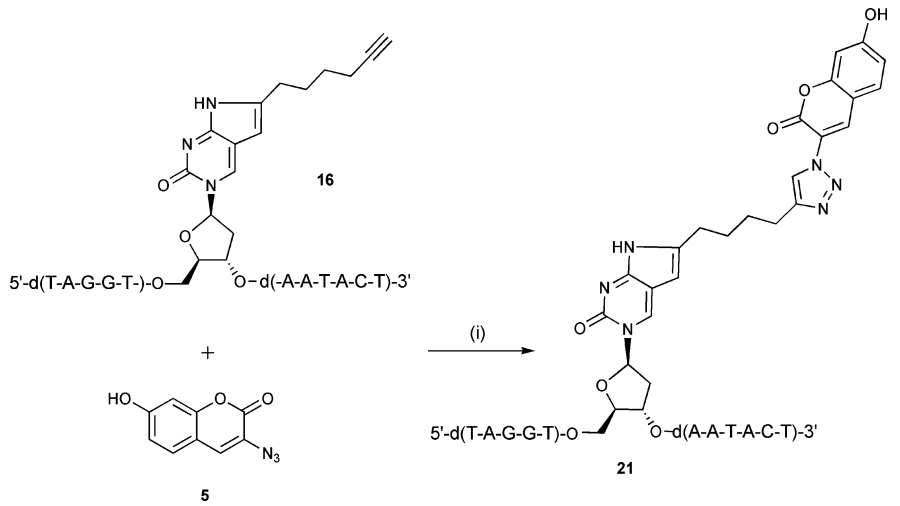

Scheme 8 *Reagents and conditions*: (i) $CuSO_4$–TBTA (1:1), TCEP, H_2O–*t*-BuOH–DMSO–THF, 16 h, r.t.

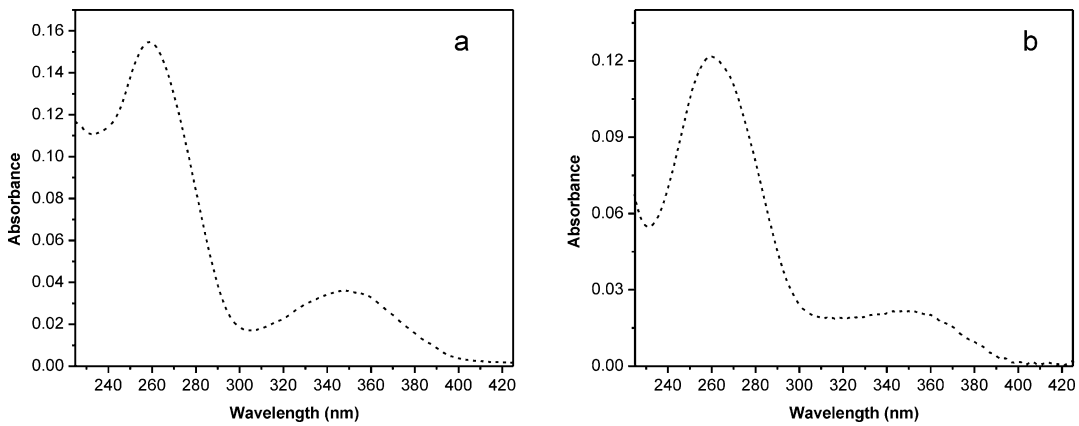

Fig. 6 UV-Vis spectra of oligonucleotide coumarin conjugates. a) 5′-d(TAG GT**31** AAT ACT), b) 5′-d(AGT ATT GA**33** CTA) measured in bi-distilled water.

oligonucleotide level. We already demonstrated the application of Huisgen–Sharpless–Meldal "click" cycloaddition for the alkynyl modified oligonucleotides on the solid-support as well as in the solution.[25,27] Here, we applied this methodology to the 12-mer oligonucleotide 5′-d(TAG GT**3** AAT ACT)-3′ (**16**) in which the central dC was replaced by **3** and performed the "click" reaction in solution. 4 OD (A_{260} units) of the purified oligonucleotide **16** and non-fluorescent 3-azido-7-hydroxycoumarin (**5**) dissolved in a *t*-BuOH–H_2O–DMSO–THF mixture were treated in the presence of 1:1 complex of $CuSO_4$–TBTA (tris(benzyltriazoylmethyl)amine) and TCEP (a water-soluble reducing agent). This resulted in the formation of the strongly fluorescent ss-oligonucleotide **21** (Scheme 8). After completion of the reaction within 16 h, the reaction mixture was centrifuged and the supernatant solution was taken, concentrated and further purified by reverse-phase HPLC (trityl-off modus; see Experimental section). The oligonucleotide dye conjugate **21** was characterized by MALDI-TOF (see ESI, Table 5†). Compared to oligonucleotide **16** the formation of the conjugate **21** was accompanied by a strong fluorescence increase. Moreover, the UV-Vis spectrum of **21** (Fig. 6a) shows a clear differentiation between the absorption of the nucleobases (260 nm) and the coumarin dye (around 350 nm), a similar differentiation was made on the oligonucleotide containing dC–coumarin nucleoside **33**[27] (Fig. 6b). Therefore, the UV-Vis measurement is a useful tool to control the performance of the "click" reaction.

Next, the fluorescence of the pyrrolo-dC nucleoside **3** as well as its coumarin conjugate **31** was studied on DNA duplexes. All fluorescence measurements of oligonucleotides were performed at a constant pH value (8.5) to ensure anion formation of the dye. As illustrated in Fig. 7a, the single-stranded oligonucleotide containing **3** displayed a strong fluorescence quenching at 462 nm upon duplex formation. Relative to the single strand **16**, the fluorescence of duplex **15**·**16** decreases by approximately 50%. We reasoned that the modified base **3** experiences less fluorescence quenching in the solvent-exposed unstructured single strand, while the base-stacked hydrophobic environment of duplex caused fluorescence quenching (Fig. 7). A similar result was observed for pyrC (**2b**) and pyrdC (**2d**) nucleosides when they are incorporated into DNA and RNA duplexes.[29]

In contrast to this, the pyrrolo-dC coumarin conjugate **31** still retains the fluorescence with a slight increase in the emission intensity after forming a duplex (Fig. 7b, Scheme 9). It is evident from previous reports that the higher energy blue fluorescence of 7-hydroxycoumarin derivatives at neutral and alkaline pH is

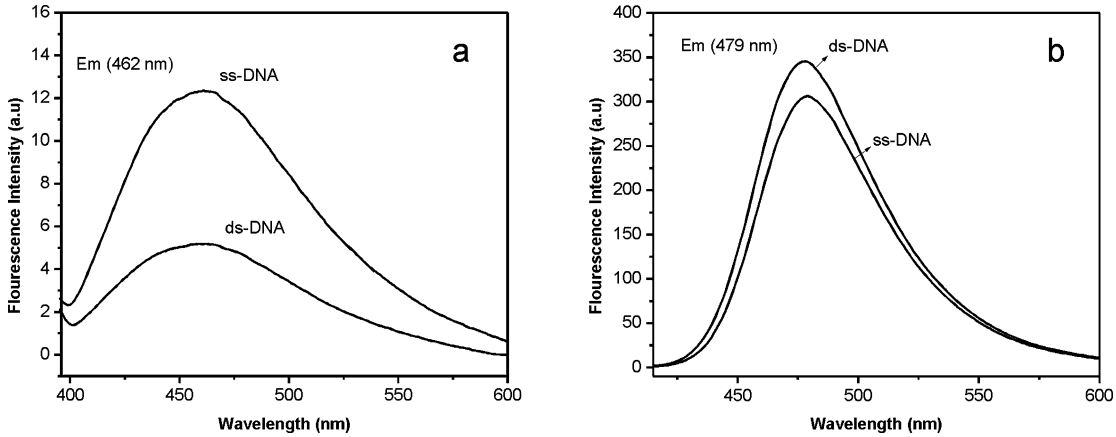

Fig. 7 Fluorescence emission a) of single-stranded **16** (2.5 μM) and duplex DNA **15**·**16** (2.5 μM + 2.5 μM), b) of click functionalized single-stranded DNA **21** (1.5 μM) and duplex DNA **15**·**21** (1.5 μM + 1.5 μM) measured in 0.1 M Tris-HCl buffer (pH 8.5).

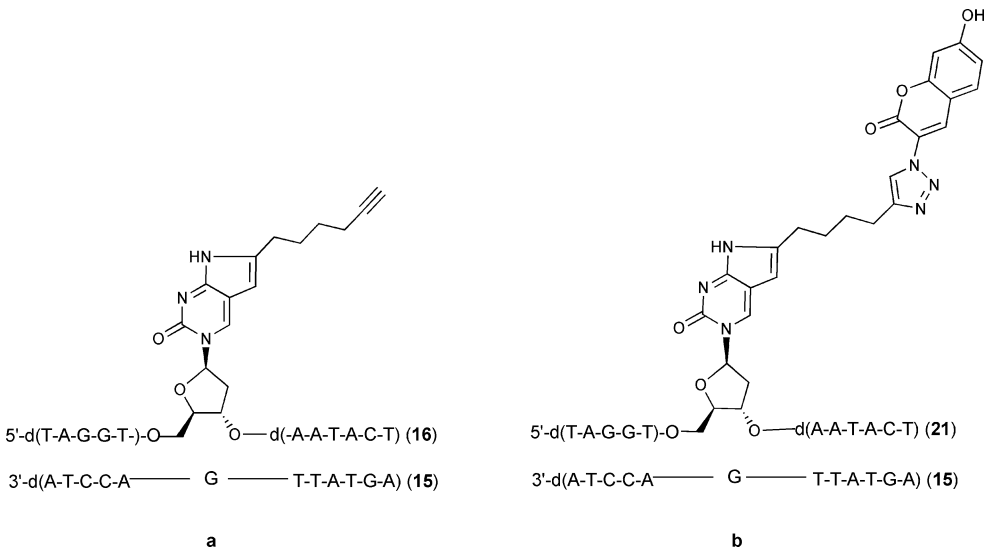

Scheme 9 a) DNA duplex containing a pyrrolo-dC nucleoside **3**, b) DNA duplex containing a pyrrolo-dC–coumarin conjugate **31**.

due to the formation of the phenolate anion. The pK_a value of 7-hydroxycoumarin was found to be in the range of 8,[46] while the presence of electron-donating groups at the 3-position influences this value. In order to confirm this, the pK_a value of 7-hydroxycoumarin of nucleoside **31** was determined UV-spectrophotometrically[48] from pH 1.5 to 11.0 at 220–350 nm and found to be in the range of 6.5. From the previous reports the pK_a of pyrC **2b** appears to be <4, slightly lower than cytosine's pK_a of 4.2.[29] From these results we can conclude that apart from the restricted freedom of the major groove coumarin dye in DNA duplex, other factors such as generation of negatively charged phenolate anion of coumarin hydroxyl group also play an important role in the fluorescence increase. It is assumed that the coumarin tether protrudes stretched-out from the major groove of the double helix and does not fold back owing to the charge repulsion between the negatively charged dye and the phosphodiester backbone. Such interactions are more predominant in duplex DNA rather than the single strand (Fig. 7b).

To determine the fluorescence characteristics of pyrdC (**3**) and its coumarin conjugate **31** in single-stranded DNA, the enzymatic hydrolysis of oligonucleotides **16** and **21** was performed using snake venom phosphodiesterase followed by alkaline phosphate and their fluorescence emission was recorded at different time intervals (Fig. 8). In the case of oligonucleotide containing pyrdC (**3**) a strong enhancement in the fluorescence emission at 466 nm was observed after complete enzymatic digestion, when excited at 347 nm, whereas the oligonucleotide with pyrdC–coumarin conjugate experiences a strong fluorescence quenching at an emission wavelength of 478 nm, when excited at 395 nm.

Based on the above results, it is apparent that the pyrrolo-dC base of **31** strongly quenches the fluorescence of the coumarin dye attached to it, unlike its open-chain derivative **33**. A similar quenching was observed for the related 7-deazapurine nucleosides.[27] The quenching is small when the pyrdC moiety of the conjugate is part of the oligonucleotide stack, while the generation of the free monomeric coumarin dye conjugate **31** formed after enzymatic hydrolysis leads to the quenching of the dye fluorescence. Apparently, in this situation, the dye and modified base (the 7-deazapurine moiety) can come in close proximity either by back-folding or by dimer formation. The excited coumarin

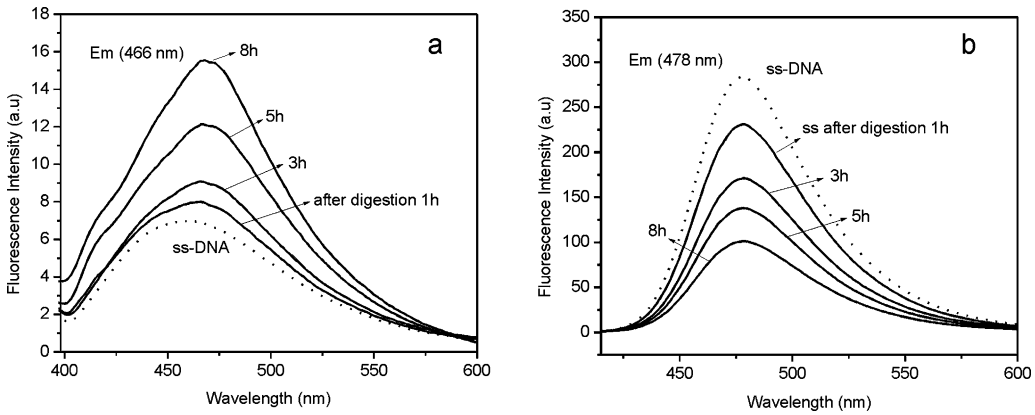

Fig. 8 Enzymatic digestion a) of 1.5 μM single-stranded oligonucleotide **16** b) of 1.5 μM single-stranded oligonucleotide **21** with snake venom phosphodiesterase followed by alkaline phosphatase in 0.1 M Tris-HCl buffer (pH 8.5) at 37 °C.

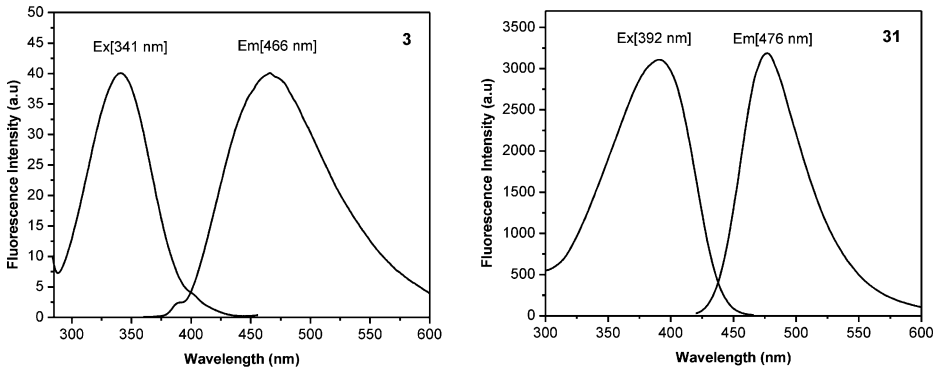

Fig. 9 The emission and excitation spectra of the pyrrolo-dC nucleoside **3** and the pyrrolo-dC coumarin conjugate **31** measured in 0.1 M Tris-HCl buffer (pH 8.5).

serves as an electron acceptor and the nucleobase as a ground-state donor.[43]

Conclusions and outlook

When the pyrdC (**3**) derivative bearing an alkynyl side chain is incorporated into DNA, it forms as stable base pair with dG as the non-functionalized pyrdC and shows a good mismatch discrimination against the canonical nucleosides (dG > dT > dA > dC). The presence of the terminal acetylene group in **3** enhances the stability of DNA duplexes opposite to canonical nucleosides, when compared with 2′-deoxycytidine. The open-chain dC derivative **4** is found to be more duplex-stabilizing than that of pyrdC. The terminal alkynyl group of compound **3** allows the functionalization with almost any azido reporter when applying the Huisgen–Sharpless–Meldal "click" chemistry. Here, the non-fluorescent coumarin azide **5** was studied to generate the highly fluorescent coumarin conjugate **31**, the reaction studied on the nucleoside and the oligonucleotide level thereby generating two fluorescent dye reporters. In ss-oligonucleotides one (pyrdC) is part of the base stack while the other (coumarin) is free, protruding into the solvent. Enzymatic phosphodiester hydrolysis of an oligonucleotide containing pyrdC (**3**) or the conjugate **31** resulted in a strong fluorescence increase of the pyrdC fluorescence while the coumarin dye became quenched during monomer formation. This can be explained by electron transfer from the pyrrolo[2,3-*d*]pyrimidine system to the coumarin dye, a phenomenon which is not observed when the nucleobase unit of **31** is part of an oligonucleotide. However, the local environment of the ionisable dye might have an influence on the dye deprotonation when it is near to the DNA backbone or liberated into the solution after enzymatic digestion. Among the two fluorescent dye moieties the coumarin shows much stronger fluorescence than the pyrdC moiety (Fig. 9). The two-dye reporter system has the potential to be used in cellular uptake studies employing copper-mediated or copper-free click chemistry.[49]

Experimental

General

All chemicals were purchased from Acros, Aldrich, Sigma, or Fluka (Sigma-Aldrich Chemie GmbH, Deisenhofen, Germany). Solvents were of laboratory grade. Thin layer chromatography (TLC): aluminium sheets, silica gel 60 F_{254}, 0.2 mm layer (VWR International, Darmstadt, Germany). Column flash chromatography (FC): silica gel 60 (VWR International, Darmstadt, Germany) at 0.4 bar; Sample collection with an UltroRac II fractions collector (LKB Instruments, Sweden). UV spectra: U-3200 spectrometer (Hitachi, Tokyo, Japan); λ_{max} (ε) in nm. NMR Spectra: Avance-250 or Avance-300 spectrometers (Bruker, Karlsruhe, Germany), at 250.13 or 300.15 MHz for ^{1}H and ^{13}C; δ in ppm relative to Me_4Si as internal standard, or external 85% H_3PO_4 for ^{31}P. The

J values are in Hz. Elemental analyses were performed by Mikroanalytisches Laboratorium Beller (Göttingen, Germany). Electron spray ionization (ESI) MS for the nucleosides: Bruker-Daltonics-MicroTOF spectrometer with loop injection (Bremen, Germany).

Fluorescence measurements. All measurements were done in bi-distilled water at 20 °C. Absorption spectra were measured with a Cary 100 Bio UV-visible spectrophotometer. In order to avoid inner filter effects the sample was not allowed to exceed 0.1 at the excitation wavelength using standard quartz cuvettes with a path length of 1 cm. Fluorescence spectra were recorded in the wavelength range between 320 and 600 nm using the Fluorescence Spectrophotometer F-2500 (Hitachi, Tokyo, Japan). For all calculations the water background was subtracted from the sample. The fluorescence quantum yields were determined using quinine sulfate in 0.1 N H_2SO_4 (fluorescence quantum yield 0.53)[30] as a standard with the following relation:

$$\Phi_{\text{f.sample}} = \Phi_{\text{f.standard}} \times (F_{\text{sample}}/F_{\text{standard}}) \times (A_{\text{standard}}/A_{\text{sample}}),$$

where $\Phi_{\text{f.sample}}$ is the unknown fluorescence quantum yield of the fluorophore, F is the integrated fluorescence intensity; A is the absorbance in 1 cm cuvettes and does not exceed 0.1 at and above the excitation wavelength.

Synthesis, purification and characterization of oligonucleotides

The oligonucleotide synthesis was performed on a DNA synthesizer, model ABI 392–08 (Applied Biosystems, Weiterstadt, Germany) at 1 μmol scale using the phosphoramidites following the synthesis protocol for 3′-cyanoethyl phosphoramidites (user's manual for the 392 DNA sythesizer, Applied Biosystems, Weiterstadt, Germany). The coupling efficiency was always higher than 95%. After cleavage from the solid support the oligonucleotides were deprotected with 25% aqueous NH_3 for 14–16 h at 60 °C. The purification of the 5′-*O*-(dimethoxytrityl)oligomers was carried out on reverse-phase HPLC (Merck-Hitachi-HPLC: 250 × 4 mm RP-18 column with the following gradient system [A: 0.1 M (Et_3NH)OAc (pH 7.0)/MeCN 95:5 and B: MeCN]; gradient: 3 min 20% B in A, 12 min 20–50% B in A and 25 min 20% B in A with a flow rate of 1 ml min^{-1}. The purified 'trityl-on' oligonucleotides were treated with 2.5% dichloroacetic acid in CH_2Cl_2 for 5 min at 0 °C to remove the 4,4′-dimethoxytrityl residues. The detritylated oligomers were purified again by reverse-phase HPLC (gradient: 0–20 min 0–20% B in A, flow rate 1 ml min^{-1}). The purification of click functionalized oligonucleotide **21** was performed in the trityl-off modus by reverse-phase HPLC (gradient: 0–25 mins 0–30% B in A, flow rate 0.8 ml min^{-1}). The oligomers were desalted on a short column (RP-18, silica gel) and lyophilized on a Speed-Vac evaporator to yield colorless solids which were frozen at −24 °C.

Melting curves were measured with a Cary-1/3 UV/VIS spectrophotometer (Varian, Australia) equipped with a Cary thermo-electrical controller. The temperature was measured continuously in the reference cell with a Pt-100 resistor, and the thermodynamic data of duplex formation were calculated by the Meltwin 3.0 program. Cary 100 Bio UV-Vis spectrophotometer was used for the UV-melting curves of oligonucleotides (Table 2) with a heating rate of 1 °C.

The enzymatic hydrolysis of the oligonucleotides was performed with snake-venom phosphodiesterase (EC 3.1.15.1, *Crotallus adamanteus*) and alkaline phosphatase (EC 3.1.3.1, *Escherichia coli* from Roche Diagnostics GmbH, Germany) in 0.1 M Tris-HCl buffer (pH 8.5), which was carried out on reverse-phase HPLC (RP-18, at 260 nm) by gradient: 0.1 M (Et_3NH)OAc (pH 7.0)/MeCN (95:5) with a flow rate of 0.7 ml min^{-1} showing the peaks of the modified and unmodified nucleosides. Quantification of the constituents was made on the basis of the peak areas, which were divided by the extinction coefficients of the nucleosides [(ε_{260}): dT 8800, dC 7300, dA 15 400, dG 11 700, **3** 4100 (MeOH)]. The molecular masses of the oligonucleotides were determined by MALDI-TOF Biflex-III mass spectrometry (Bruker Saxonia, Leipzig, Germany) and Applied Biosystems Voyager DE PRO with 3-hydroxypicolinic acid (3-HPA) as a matrix. The detected masses were identical to the calculated values (ESI, Table 5†).

3-(2-Deoxy-β-D-*erythro*-pentofuranosyl)-3,7-dihydro-6-hexynyl-2*H*-pyrrolo[2,3-*d*]pyrimidin-2-one (3). A solution of compound **7** (180 mg, 0.54 mmol)[28] in 25% aqueous ammonium hydroxide (30 ml) was stirred at r.t. overnight. The solvent was evaporated and the residue was applied to flash chromatography (FC) (silica gel, column 8 × 2 cm, CH_2Cl_2–MeOH, 9:1). The main zone afforded **3** (162 mg, 90%) as a yellowish solid. (Found: C, 61.80; H, 6.27; N, 12.58%. $C_{17}H_{21}N_3O_4$ requires C, 61.62; H, 6.39; N, 12.68%); TLC (silica gel, CH_2Cl_2–MeOH, 9:1): R_f 0.34; λ_{max} (MeOH)/nm 229 (ε/dm^3 mol^{-1} cm^{-1} 27 500), 262 (4 200), 344 (4 100); δ_H (250.13 MHz; [d_6]DMSO; Me_4Si) 1.43–1.71 (4 H, m, 2 × CH_2), 2.01 (1 H, m, 2′-H_α), 2.15–2.31 (3 H, m, 2′-H_β, CH_2), 2.54 (2 H, m, CH_2), 2.75 (1 H, s, C≡CH), 3.63 (2 H, m, 5′-H), 3.86 (1 H, m, 4′-H), 4.23 (1 H, m, 3′-H), 5.10 (1 H, t, *J* 4.71, 5′-OH), 5.25 (1 H, d, *J* 3.46, 3′-OH), 5.91 (1 H, s, 5-H), 6.25 (1 H, t, *J* 6.15, 1′-H), 8.50 (1 H, s, 4-H), 11.1 (1 H, s, NH).

3-[2-Deoxy-5-*O*-(4,4′-dimethoxytriphenylmethyl)-β-D-*erythro*-pentofuranosyl]-6-(hexynyl)-furo[2,3-*d*]pyrimidin-3*H*-2-one (9). *Method A*: Compound **7** (470 mg, 1.41 mmol) was dried by repeated co-evaporation with anhydrous pyridine (2 × 10 ml) before dissolving in anhydrous pyridine (10 ml). 4,4′-Dimethoxytriphenylmethyl chloride (610 mg, 1.80 mmol) was added in three portions to the remaining solution at r.t. under stirring for 6 h. The reaction was quenched by the addition of MeOH (2 ml) and the mixture was evaporated to dryness. The reaction mixture was dissolved in CH_2Cl_2 (2 × 50 ml) and extracted with 5% aqueous sodium bicarbonate (100 ml) followed by water (80 ml), dried over Na_2SO_4 and then evaporated. Purification by FC (silica gel, column 15 × 3 cm) eluting with CH_2Cl_2–MeOH, 95:5 to give a colorless foam of **9** (0.73 g 81%). *Method B*: To a solution of Compound **8** (200 mg, 0.31 mmol) in 15 ml (MeOH–Et_3N, 7:3) was added CuI (12 mg, 0.063 mmol) and refluxed for 5 h. The solvent was evaporated *in vacuo* and the crude product was purified by FC (silica gel, column 8 × 2 cm, CH_2Cl_2–acetone 7:3) afforded 170 mg (85%) of **9**. (Found: C, 72.03; H, 6.20, N, 4.30%. $C_{38}H_{38}N_2O_7$ requires C, 71.91; H, 6.03; N, 4.41%); TLC (silica gel, CH_2Cl_2–MeOH, 9:1): R_f 0.74; λ_{max} (MeOH)/nm 233 (ε/dm^3 mol^{-1} cm^{-1} 32 000), 275 (3 600), 333 (6 900); δ_H (250.13 MHz; [d_6]DMSO; Me_4Si) 1.45–150 (2 H, m, CH_2), 1.62–1.65 (2 H, m, CH_2), 2.08–2.22 (3 H, m, 2′-H_α, CH_2), 2.39–2.63 (3 H, m, 2′-H_β, CH_2), 2.76 (1 H, s, C≡CH), 3.25–3.29 (2 H, m, 5′-H), 3.73 (6 H, s, 2 × OCH_3), 4.01 (1 H, m, 4′-H)), 4.38

(1 H, m, 3′-H), 5.42 (1 H, d, *J* 4.60, 3′-OH), 5.65 (1 H, s, 5-H), 6.14 (1 H, t, *J* 5.31, 1′-H), 6.87–7.38 (m, H–arom), 8.53 (1 H, s, 4-H).

3-[2-Deoxy-5-*O*-(4,4′-dimethoxytriphenylmethyl)-β-D-*erythro*-pentofuranosyl]-6-(hexyl)-furo[2,3-*d*]pyrimidin-3*H*-2-one (12). As described above with compound **11** (400 mg, 0.62 mmol), MeOH–Et_3N, 7:3 (30 ml) and CuI (24 mg, 0.126 mmol). Purification by FC (silica gel, column 15 × 3 cm, CH_2Cl_2–acetone 7:3) gave a colorless foam of **12** (348 mg, 87%). (Found: C, 71.35; H, 6.61; N, 4.36%. $C_{38}H_{42}N_2O_7$ requires C 71.45; H, 6.63; N, 4.39%); TLC (silica gel, CH_2Cl_2–MeOH, 9:1): R_f 0.67; λ_{max} (MeOH)/nm 233 (ε/dm^3 mol^{-1} cm^{-1} 27 000), 275 (3 000), 334 (5 400); δ_H (250.13 MHz; [d_6]DMSO; Me_4Si) 0.86 (3 H, CH_3), 1.15–1.54 (8 H, m, CH_2), 2.11 (2 H, m, 2′-H), 2.44 (2 H, m, CH_2), 3.11 (2 H, m, 5′-H), 3.73 (6 H, s, 2 × OCH_3), 4.0 (1 H, m, 4′-H), 4.39 (1 H, m, 3′-H), 5.42 (1 H, d, *J* 3.56, 3′-OH), 5.63 (1 H, s, 5-H), 6.14 (1 H, t, *J* 5.31, 1′-H), 6.87–7.36 (m, H–arom), 8.55 (1H, s, 4-H).

3-[2-Deoxy-5-*O*-(4,4′-dimethoxytriphenylmethyl)-β-D-*erythro*-pentofuranosyl]-6-(hexynyl)-furo[2,3-*d*]pyrimidin-3*H*-2-one-3′-(2-cyanoethyl-*N*,*N*-diisopropylphosphoramidite (10). A stirred solution of **9** (170 mg, 0.27 mmol) in anhydrous CH_2Cl_2 (5 ml) was preflushed with argon and treated with (i-Pr)$_2$EtN (93 µl, 0.54 mmol) followed by (2-cyanoethyl)diisopropylphosphoramidochloridite (118 µl, 0.54 mmol). After stirring for 45 min at r.t. the solution was diluted with CH_2Cl_2 (30 ml) and extracted with 5% aqueous $NaHCO_3$ solution (20 ml). The organic layer was dried (Na_2SO_4), filtered and evaporated. FC (silica gel, column 10 × 3 cm, CH_2Cl_2–acetone, 9:1) gave colorless foam of **10** (140 mg, 63%). TLC (silica gel, CH_2Cl_2–acetone, 95:5): R_f 0.60. ^{31}P NMR ($CDCl_3$): 150.12, 149.74.

3-[2-Deoxy-5-*O*-(4,4′-dimethoxytriphenylmethyl)-β-D-*erythro*-pentofuranosyl]-6-(hexyl)-furo[2,3-*d*]pyrimidin-3*H*-2-one 3′-(2-cyanoethyl-*N*,*N*-diisopropylphosphor-amidite (13). As described for **10**, with **12** (200 mg, 0.31 mmol), (i-Pr)$_2$EtN (100 µl, 0.58 mmol) and 2-cyanoethyl-diisopropylphosphoramidochloridite (94 µl, 0.43 mmol). FC (silica gel, column 10 × 3 cm, CH_2Cl_2–acetone 95:5) afforded **13** as a colorless foam (160 mg, 61%). TLC (silica gel, CH_2Cl_2–acetone 9:1): R_f 0.70. ^{31}P NMR ($CDCl_3$): 150.88, 150.07.

Preparation of the conjugate 30 from nucleoside 7 and 3-azido-7-hydroxycoumarin (5)

To a solution of compound **7** (120 mg, 0.36 mmol) and 3-azido-7-hydroxycoumarin (**5**; 86.5 mg, 0.43 mmol) in THF–H_2O–*t*-BuOH, 3:1:1, (4 ml), was added sodium ascorbate (312 µl, 0.31 mmol) of a freshly prepared 1 M solution in water, followed by the addition of copper(II) sulfate pentahydrate 7.5% in water (260 µl, 0.078 mmol). The emulsion was stirred for 24 h at r.t. evaporated, and applied to FC (silica gel, column 10 × 3 cm, CH_2Cl_2–MeOH, 88:12). From the main zone compound **30** (158 mg, 82%) was isolated as a yellowish solid. TLC (silica gel, CH_2Cl_2–MeOH, 9:1): R_f 0.41. λ_{max} (MeOH)/nm 342 (ε/dm^3 mol^{-1} cm^{-1} 22 000); δ_H (250.13 MHz; [d_6]DMSO; Me_4Si) 1.70 (4 H, m, 2 × CH_2), 2.06 (1 H, m, 2′-H_α), 2.39 (1 H, m, 2′-H_β), 2.74 (4 H, m, 2 × CH_2), 3.63 (2 H, m, 5′-H), 3.89 (1 H, m, 4′-H), 4.22 (1 H, m, 3′-H), 5.12 (1 H, 5′-OH), 5.28 (1 H, 3′-OH), 6.16 (1 H, t, *J* 6.12, 1′-H), 6.45 (1 H, s, 5-H), 6.84 (1 H-arom, d, *J* 2.05), 6.87–6.92 (1 H-arom, dd, *J* 8.50), 7.74 (1 H-arom, d, *J* 8.60), 8.31 (1 H-arom, s, C=CH), 8.55 (1 H-arom, s), 8.67 (1 H, s, 4-H), 10.8 (1 H, s, OH). (Found: ESI-HR-MS: 558.16 ([M + Na])$^+$, $C_{26}H_{25}N_5O_8$; requires 535.17).

Preparation of the conjugate 31 from nucleoside 3 and 3-azido-7-hydroxycoumarin (5)

As described for **30** a solution of **3** (80 mg, 0.24 mmol), 3-azido-7-hydroxycoumarin (**5**; 57 mg, 0.28 mmol) in THF–H_2O–*t*-BuOH, 3:1:1 (4 ml) was stirred at r.t. for 30 h with 1 M aqueous sodium ascorbate (210 µl, 0.21 mmol) and copper(II) sulfate pentahydrate (173 µl, 0.052 mmol of a 7.5% stock solution in water). The solvent was evaporated and applied to FC (silica gel, column 10 × 3 cm, CH_2Cl_2–MeOH 85:15) to afford compound **31** (110 mg, 85%) as a yellowish solid. TLC (silica gel, CH_2Cl_2–MeOH, 88:12): R_f 0.52. λ_{max} (MeOH)/nm 220 (ε/dm^3 mol^{-1} cm^{-1} 25 000), 346 (13 000); δ_H (300.15 MHz; [d_6]DMSO; Me_4Si) 1.70 (4 H, m, 2 × CH_2), 2.03 (1 H, m, 2′-H_α), 2.30 (1 H, m, 2′-H_β), 2.58–2.74 (4 H, m, 2 × CH_2), 3.62 (2 H, m, 5′-H), 3.87 (1 H, m, 4′-H), 4.22 (1 H, m, 3′-H), 5.10 (1 H, 5′-OH), 5.25 (1 H, 3′-OH), 6.0 (1 H, s, 5-H), 6.24 (1 H, t, *J* 6.2, 1′-H), 6.84 (1 H-arom, d), 6.88–6.92 (1 H-arom, dd, *J* 8.41), 7.74 (1 H-arom, d, *J* 8.70), 8.31 (1 H-arom, s, C=CH), 8.49 (1 H, s, 4-H), 8.55 (1 H-arom, s), 10.9 (1 H, s, OH), 11.1 (1 H, s, NH). (Found: ESI-HR-MS: 557.18 ([M + Na])$^+$, $C_{26}H_{26}N_6O_7$; requires 534.19).

Preparation of the conjugate 32 from nucleoside 6 and 3-azido-7-hydroxycoumarin (5)

As described for **30** with **6** (100 mg, 0.30 mmol), 3-azido-7-hydroxycoumarin (**5**; 74 mg, 0.36 mmol) in THF–H_2O–*t*-BuOH, 3:1:1 (4 ml) was stirred at r.t for 10 h with 1 M aqueous sodium ascorbate (300 µl, 0.30 mmol), copper(II) sulfate pentahydrate (260 µl, 0.078 mmol of a 7.5% stock solution in water). The solvent was evaporated and applied to FC (silica gel, column 10 × 3 cm, CH_2Cl_2–MeOH 90:10) to afford compound **32** (130 mg, 81%) as a yellowish solid. TLC (silica gel, CH_2Cl_2–MeOH, 9:1): R_f 0.30. λ_{max} (MeOH)/nm 297 (ε/dm^3 mol^{-1} cm^{-1} 13 000), 346 (17 000); δ_H (300.15 MHz; [d_6]DMSO; Me_4Si) 1.60–1.80 (4 H, m, 2 × CH_2), 2.11 (2 H, m, 2′-H), 2.42 (2 H, m, CH_2), 2.77 (2 H, m, CH_2), 3.48 (2 H, m, 5′-H), 3.78 (1 H, m, 4′-H), 4.22 (1 H, m, 3′-H), 5.10 (1 H, 5′-OH), 5.23 (1 H, 3′-OH), 6.10 (1 H, t, *J* 6.45, 1′-H), 6.84 (1 H-arom, d), 6.88–6.92 (1 H-arom, dd, *J* 8.58), 7.74 (1 H-arom, d, *J* 8.70), 8. 12 (1 H, s, 4-H), 8.31 (1 H-arom, s, C=CH), 8.55 (1 H-arom, s), 10.9 (1 H, s, OH), 11.5 (1 H, s, NH). (Found: ESI-HR-MS: 558.16 ([M + Na])$^+$, $C_{26}H_{25}N_5O_8$; requires 535.17).

Preparation of the conjugate 33 from nucleoside 4 and 3-azido-7-hydroxycoumarin (5)

Compound **33** was synthesised from **4** (60 mg, 0.18 mmol) according to the above method. Compound **33** (59 mg, 61%) was isolated from the main zone as a yellowish solid. TLC (silica gel, CH_2Cl_2–MeOH, 9:1): R_f 0.15. λ_{max} (MeOH)/nm 345 (ε/dm^3 mol^{-1} cm^{-1} 9 500); δ_H (300.15 MHz; [d_6]DMSO; Me_4Si) 1.61–1.77 (4 H, m, 2 × CH_2), 1.98–2.10 (2 H, m, 2′-H), 2.46 (2 H, m, CH_2), 2.75 (2 H, m, CH_2), 3.56 (2 H, m, 5′-H), 3.78 (1 H, m, 4′-H), 4.20 (1 H, m, 3′-H), 5.06 (1 H, 5′-OH), 5.20 (1 H, 3′-OH), 6.10 (1 H, t, *J* 6.18, 1′-H), 6.84 (1 H-arom, d), 6.74 (1 H, s, NH_a), 6.85 (1 H-arom, d), 6.89–6.92 (1 H-arom, dd, *J* 8.46), 7.71 (1 H, s, NH_b),

7.74 (1 H-arom, d), 8.08 (1 H, C(6)), 8.31 (1 H-arom, s, C=CH), 8.55 (1 H-arom, s), 10.9 (1 H, s, OH). (Found: ESI-HR-MS: 557.18 ($[M + Na]^+$, $C_{26}H_{26}N_6O_7$; requires 534.19).

Copper(I)-catalyzed [3 + 2] cycloaddition of the oligonucleotide 16 with coumarin azide 5. To the single-stranded oligonucleotide **16** (4 A_{260} units, 31 nmol), a 1:1 complex of $CuSO_4$–TBTA ligand (35 µl of a 20 mM stock solution in *t*-BuOH–H_2O 1:9), tris(carboxyethyl)phosphine (TCEP; 35 µl of a 20 mM stock solution in H_2O), 3-azido-7-hydroxycoumarin (**5**; 50 µl of a 20 mM stock solution in THF) and 35 µl DMSO was added and the reaction mixture stirred at r.t. for 16 h. The reaction mixture was concentrated in a speed vac and dissolved in 1 ml bi-distilled water and centrifuged for 20 min at 12 000 rpm. The supernatant solution was collected and further purified by reverse-phase HPLC in the trityl-off modus (for details see above) to give **21**. MALDI-TOF: (ESI, Table 5†).

Acknowledgements

We thank Mrs S. Budow and P. Chittepu for measuring the NMR spectra, Dr K. I. Shaikh (Muenster) and Dr T. Koch from Roche Diagnostics GmbH, Penzberg, Germany for the MALDI-TOF spectra, Mrs E. Michalek and Mr Tran for the oligonucleotide syntheses and Mr P. Leonard for reading the manuscript. Financial support by ChemBiotech, Münster, and the BMBF is gratefully acknowledged.

References

1 (*a*) N. J. Greco and Y. Tor, *Tetrahedron*, 2007, **63**, 3515–3527; (*b*) D. C. Ward and E. Reich, *J. Biol. Chem.*, 1969, **244**, 1228–1237.
2 F. Seela, H. Steker, H. Driller and U. Bindig, *Liebigs Ann. Chem.*, 1987, 15–19.
3 F. Seela and H. Steker, *Liebigs Ann. Chem.*, 1984, 1719–1730.
4 F. Seela, Y. Chen, U. Bindig and Z. Kazimierczuk, *Helv. Chim. Acta*, 1994, **77**, 194–202.
5 J. A. Secrist III, J. R. Barrio, N. J. Leonard and G. Weber, *Biochemistry*, 1972, **11**, 3499–3506.
6 F. Seela, E. Schweinberger, K. Xu, V. R. Sirivolu, H. Rosemeyer and E. M. Becker, *Tetrahedron*, 2007, **63**, 3471–3482.
7 S. C. Srivastava, S. K. Raza and R. Misra, *Nucleic Acids Res.*, 1994, **22**, 1296–1304.
8 W. Zhang, R. Rieger, C. Iden and F. Johnson, *Chem. Res. Toxicol.*, 1995, **8**, 148–156.
9 J. Woo, R. B. Meyer, Jr and H. B. Gamper, *Nucleic Acids Res.*, 1996, **24**, 2470–2475.
10 D. A. Berry, K.-Y. Jung, D. S. Wise, A. D. Sercel, W. H. Pearson, H. Mackie, J. B. Randolph and R. L. Somers, *Tetrahedron Lett.*, 2004, **45**, 2457–2461.
11 D. Loakes, D. M. Brown, S. A. Salisbury, M. G. McDougall, C. Neagu, S. Nampalli and S. Kumar, *Helv. Chim. Acta*, 2003, **86**, 1193–1204.
12 C. McGuigan, R. N. Pathirana, G. Jones, G. Andrei, R. Snoeck, E. De Clercq and J. Balzarini, *J. Antiviral Chem Chemother.*, 2000, **11**, 343–348.
13 C. McGuigan, C. J. Yarnold, G. Jones, S. Velázquez, H. Barucki, A. Brancale, G. Andrei, R. Snoeck, E. De Clercq and J. Balzarini, *J. Med. Chem.*, 1999, **42**, 4479–4484.
14 H. Inoue, A. Imura and E. Ohtsuka, *Nippon Kagaku Kaishi.*, 1987, **7**, 1214–1220.
15 T. Shibata, N. J. Buurma, J. A. Brazier, P. Thompson, I. Haq and D. M. Williams, *Chem. Commun.*, 2006, 3516–3518.
16 P. Chen and C. He, *J. Am. Chem. Soc.*, 2004, **126**, 728–729.
17 C. Dash, J. W. Rausch and S. F. G. Le Grice, *Nucleic Acids Res.*, 2004, **32**, 1539–1547.
18 C. Liu and C. T. Martin, *J. Mol. Biol.*, 2001, **308**, 465–475.
19 C. Liu and C. T. Martin, *J. Biol. Chem.*, 2002, **277**, 2725–2731.
20 R. T. Ranasinghe, D. A. Rusling, V. E. C. Powers, K. R. Fox and T. Brown, *Chem. Commun.*, 2005, 2555–2557.
21 A. A. Martí, S. Jockusch, Z. Li, J. Ju and N. J. Turro, *Nucleic Acids Res.*, 2006, **34**, e50.
22 R. Huisgen, in *1,3-Dipolar Cycloaddition Chemistry*, ed. A. Padwa, Wiley, New York, 1984.
23 V. V. Rostovtsev, L. G. Green, V. V. Fokin and K. B. Sharpless, *Angew. Chem, Int. Ed.*, 2002, **41**, 2596–2599.
24 C. W. Tornøe, C. Christensen and M. Meldal, *J. Org. Chem.*, 2002, **67**, 3057–3064.
25 F. Seela and V. R. Sirivolu, *Helv. Chim. Acta*, 2007, **90**, 535–552.
26 F. Seela and V. R. Sirivolu, *Chem. Biodiv.*, 2006, **3**, 509–514.
27 F. Seela, V. R. Sirivolu and P. Chittepu, *Bioconjugate Chem.*, 2008, **19**, 211–224.
28 S. Srinivasan, C. McGuigan, G. Andrei, R. Snoeck, E. De Clercq and J. Balzarini, *J. Bioorg. Med. Chem. Lett.*, 2001, **11**, 391–393.
29 R. A. Tinsley and N. G. Walter, *RNA*, 2006, **12**(3), 522–529.
30 A. N. Fletcher, *Photochem. Photobiol.*, 1969, **9**, 439–444.
31 T. S. Seo, Z. Li, H. Ruparel and J. Ju, *J. Org. Chem.*, 2003, **68**, 609–612.
32 R. L. Weller and S. R. Rajski, *Org. Lett.*, 2005, **7**, 2141–2144.
33 J. Gierlich, G. A. Burley, P. M. E. Gramlich, D. M. Hammond and T. Carell, *Org. Lett.*, 2006, **8**, 3639–3642.
34 S. Dedola, S. A. Nepogodiev and R. A. Field, *Org. Biomol. Chem.*, 2007, **5**, 1006–1017.
35 V. D. Bock, H. Hiemstra and J. H. van Maarseveen, *Eur. J. Org. Chem.*, 2006, 51–68.
36 W. H. Binder and C. Kluger, *Curr. Org. Chem.*, 2006, **10**, 1791–1815.
37 D. D. Díaz, S. Punna, P. Holzer, A. K. McPherson, K. B. Sharpless, V. V. Fokin and M. G. Finn, *J. Polym. Sci. Part A*, 2004, **42**, 4392–4403.
38 Q. Wang, T. R. Chan, R. Hilgraf, V. V. Fokin, K. B. Sharpless and M. G. Finn, *J. Am. Chem. Soc*, 2003, **125**, 3192–3193.
39 (*a*) K. E. Beatty, F. Xie, Q. Wang and D. A. Tirrell, *J. Am. Chem. Soc.*, 2005, **127**, 14150–14151; (*b*) P. Kočalka, N. K. Andersen, F. Jensen and P. Nielsen, *ChemBioChem*, 2007, **8**, 2106–2116.
40 K. Sivakumar, F. Xie, B. M. Cash, S. Long, H. N. Barnhill and Q. Wang, *Org. Lett.*, 2004, **6**, 4603–4606.
41 R. S. Coleman, M. A. Berg and C. J. Murphy, *Tetrahedron*, 2007, **63**, 3450–3456.
42 I. Kosiova, A. Janicova and P. Kois, *Beilstein J. Org. Chem.*, 2006, **2**, 23.
43 C. A. M. Seidel, A. Schulz and M. H. M. Sauer, *J. Phys. Chem.*, 1996, **100**, 5541–5553.
44 B. Hoffmann, B. Bernet and A. Vasella, *Helv. Chim. Acta*, 2002, **85**, 265–287.
45 A. Dondoni and A. Marra, *J. Org. Chem.*, 2006, **71**, 7546–7557.
46 D. W. Fink and W. R. Koehler, *Anal. Chem.*, 1970, **42**, 990–993.
47 R. P. Haugland, *Handbook of Fluorescent Probes and Research Chemicals*, 6th edition, Molecular Probes Inc., Eugene, OR, USA, 1996.
48 A. Albert and E. P. Serjeant, in *The Determination of Ionization Constants*, Chapman and Hall, London, 1971, pp. 44–64.
49 J. M. Baskin, J. A. Prescher, S. T. Laughlin, N. J. Agard, P. V. Chang, I. A. Miller, A. Lo, J. A. Codelli and C. R. Bertozzi, *Proc. Natl. Acad. Sci. U. S. A.*, 2007, **104**, 16793–16797.